



Proceeding Paper

An In Silico Approach for Comparative Characterization of Imidazolonepropionase from *Agrobacterium fabrum* & *Bacillus subtilis*: An Imperative Enzyme for Histidine Degradation [†]

Ishita Biswas ¹, Trishanjan Biswas ² and Debanjan Mitra ^{3,*}

¹ Department of Botany, S.B.S. Government College, Hili 733126, West Bengal, India

² Department of Sericulture, Raiganj University, Raiganj 733134, West Bengal, India

³ Department of Microbiology, The University of Burdwan, Burdwan 713104, West Bengal, India

* Correspondence: debanjanmitra267@gmail.com

[†] Presented at the 4th International Electronic Conference on Agronomy, 2–5 December 2024; Available online: <https://sciforum.net/event/IECAG2024>.

Abstract: Introduction: The third step in histidine degradation is catalysed by imidazolonepropionase. It catalyses the conversion of 4-imidazolone-5-propionic acid to produce N-formimino-L-glutamic acid by hydrolyzing the carbon-nitrogen bonds. The histidine is a very expensive amino acid inside the cell and its degradation is a very conserved process. To date, very few reports are there regarding the structure of bacterial imidazolonepropionase but no reports have been published regarding the comparative structure and sequence analysis of this enzyme from bacterial sources. Methods: An in-silico study has been done to characterize the imidazolonepropionase from gram-positive *Bacillus subtilis* and gram-negative *Agrobacterium fabrum*. Results: The sequence analysis revealed that a higher amount of charged residues are present in *Bacillus subtilis*. These charged residues help in the increment of polarity and hydrophilicity of *Bacillus subtilis*. The formation of intra-protein interactions was also high in gram-positive species. Interestingly, both species have almost equal abundance of aromatic amino acids in their sequences, but the formation of aromatic-aromatic interactions was high in *Bacillus subtilis*. Finally, the molecular dynamics simulation study revealed that imidazolonepropionase from *Bacillus subtilis* was more stable and compact than *Agrobacterium fabrum*. Conclusions: The imidazolonepropionase from *Bacillus subtilis* was more stable than *Agrobacterium fabrum*. Due to the presence of higher stable imidazolonepropionase in *Bacillus subtilis*, it can use histidine more efficiently.

Keywords: imidazolonepropionase; histidine degradation; intra-protein interactions; molecular dynamics simulation



Academic Editor: José David Flores-Félix

Published: 13 March 2025

Citation: Biswas, I.; Biswas, T.; Mitra, D. An In Silico Approach for Comparative Characterization of Imidazolonepropionase from *Agrobacterium fabrum* & *Bacillus subtilis*: An Imperative Enzyme for Histidine Degradation. *Biol. Life Sci. Forum* **2025**, *41*, 3. <https://doi.org/10.3390/blsf2025041003>

Copyright: © 2025 by the authors. Licensee MDPI, Basel, Switzerland. This article is an open access article distributed under the terms and conditions of the Creative Commons Attribution (CC BY) license (<https://creativecommons.org/licenses/by/4.0/>).

1. Introduction

Starting from bacteria to eukaryotes, one highly conserved pathway is the degradation of histidine, which is the essential amino acid inside the cell. Degradation of histidine involves consecutive participation of four enzymes namely histidase (HutH, EC 4.3.1.3), urocanase (HutU, EC 4.2.1.49), imidazolonepropionase (HutI, EC 3.5.2.7) and formimino-glutamate hydrolase (HutG, EC 3.5.3.8) and they were all operated by hut operon [1]. The main interest of our study is the enzyme imidazolonepropionase also known as imidazolone-5-propanote hydrolase, having a molecular weight of 46.6 kDa, belongs to the superfamily amidohydrolase [2]. It catalyzes the third step in the histidine degradation pathway by converting 4-imidazolone-5-propionic acid (IPA) by hydrolytic cleavage of the

carbon-nitrogen bond of it to form N-formimino-L-glutamate [3]. The flow chart of the histidine degradation pathway has been presented in Figure 1.

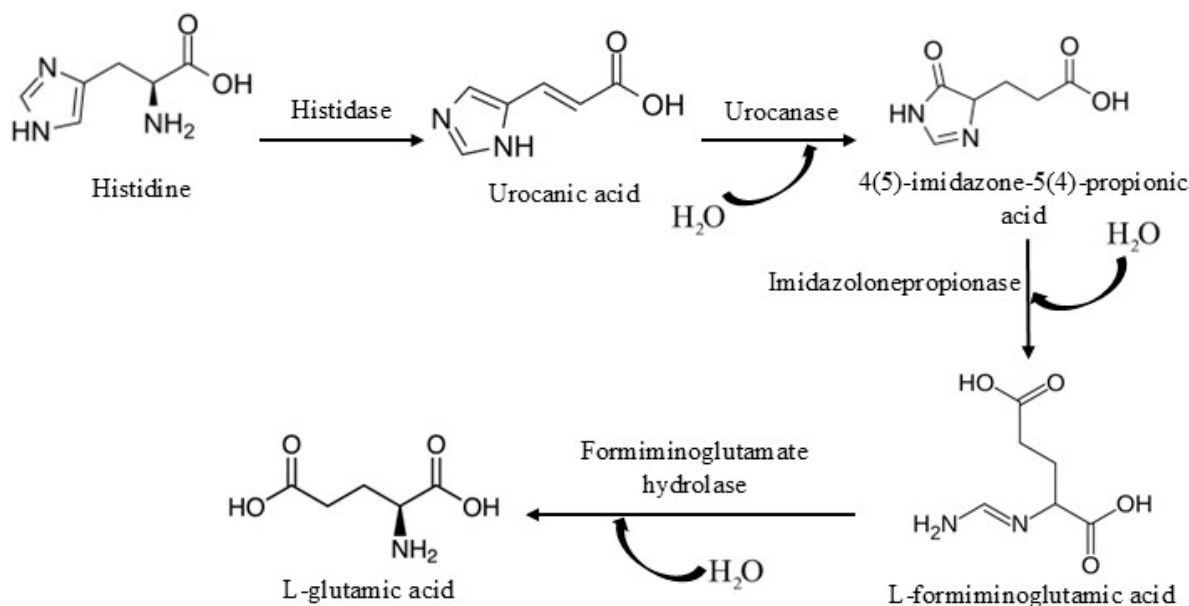


Figure 1. Degradation pathway of histidine.

The enzyme imidazolonepropionase was reported to show maximum activity at pH 7.4 [4] and the main inhibitor of the enzyme is 0.1 mM p-chloromercuribenzoate. It was further reported that the enzyme is cysteine-dependent and not a metalloprotein and could form TIM barrel [5]. Yu et al. [5] reported the crystal structures of imidazolonepropionase from *Bacillus subtilis* and the three-dimensional crystal structures of imidazolonepropionase from *Agrobacterium tumefaciens* was documented by Yu et al. [2]. In both cases the enzyme was found to possess a single metal ion ligated to the α -site. Zn²⁺ metal ions are bonded in both forms, nonetheless, Fe³⁺ is present at the active site in the structure of *Agrobacterium tumefaciens*. In the case of imidazolonepropionase of *B. subtilis*, the zinc ion forms a catalytic triad with the residues His80 and Asp271 (or His249 and Asp219) [6]. While, in *A. tumefaciens*, the organization of the active site showed the presence of Fe³⁺ metal ion, one aspartic acid (Asp331) and four histidine (His86; His88; His256, and His279) [1]. There are few reports in the literature regarding the structure of imidazolonepropionase. Still, no such reports exist regarding the sequence and structure analysis to understand the functionality of the enzyme.

In this paper, we have done an in-silico investigation on imidazolonepropionase from gram (–) *Agrobacterium fabrum* and gram (+) *Bacillus subtilis* to differentiate their sequential and structural changes.

2. Materials and Methods

2.1. Dataset

All the protein sequences of imidazolonepropionase from Gram (–) *Agrobacterium fabrum* formerly known as *Agrobacterium tumefaciens* (Q8U8Z6) and Gram (+) *Bacillus subtilis* (P42084), were extracted from the UniProt database. The crystal structure of proteins (2PUZ & 2G3F) was extracted from the RCSB PDB.

2.2. Analysis of Protein Sequences

All reviewed sequences of Imidazolonepropionase from *Agrobacterium fabrum* and *Bacillus subtilis* were subjected to multiple sequence alignment through Clustal omega for block preparation. Non-block format of sequences was used to calculate physicochemical

properties by the ProtParam server [7]. Block of sequences was used to calculate polarity, hydrophathy, and intrinsic disordered regions. To check the polarity and hydrophathy the ProtScale server was used [8].

2.3. Analysis of Protein Structures

The Imidazolonepropionase structure from *Agrobacterium fabrum* and *Bacillus subtilis* were minimized in 1000 steps through the UCSF Chimera 1.15rc along with the Amber forcefield. The CFSSP server did the Secondary structure assessment. The energy contribution of different amino acid groups was calculated by the InterProSurf server. The Ring 2.0 server identified intra-protein interactions. The identification of tunnels, cavities, and voids was done using the Mole 2.0 server [9].

2.4. Molecular Dynamic Simulations

To check the protein stability, rigidity, and compactness, molecular dynamic simulations were performed on all protein structures through GROMACS and GROMOS96 43a1 forcefield [10]. In the SPC water model with triclinic type box and NaCl salt, the energy was minimized by 5000 steps. The final run was done for 50 ns at 300 K temperature, 1 bar pressure, and 1000 frames per simulation. Properties like RMSD, RMSF, Rg, SASA, and hydrogen bonds were calculated from the simulation study.

3. Results and Discussions

3.1. Amino Acid Diversity and Secondary Structure Formation

Amino acid diversity is the building block of proteins, making proteins different across species. The Imidazolonepropionase from *A. fabrum* revealed that it has 23.73% polar-charged amino acids (Figure 2). However, the overall abundance of charged amino acids was high in *B. subtilis*. Uncharged polar amino acids have an equal presence in both species. Although the Ala amino acids showed a very higher abundance in *A. fabrum*, the overall hydrophobic residues abundance was high in imidazolonepropionase from *B. subtilis*. Bacterial growth rates can be regulated by extracellular alanine, especially in strains lacking in alanine cross-feeding [11]. However, the abundance of charged residues has a great impact on bacterial protein stability.

The incorporation of charged polar amino acids in its sequence of *B. subtilis* significantly increased its polarity. Although both species have equal amounts of uncharged polar residues, the slight abundance of charged residues in *B. subtilis* played a crucial role in polarity increment. Higher polarity significantly boosts thermostability [12]. The hydrophathy scale revealed that the imidazolonepropionase from *B. subtilis* was more hydrophilic rather than *A. fabrum*. Hydrophilic enzymes have easily interacted with aqueous medium.

Torsion angles, which are part of secondary structures, help to build sheets and helices. Protein turns and hydrophobicity also have an impact on a protein's secondary structure, leading to the formation of alternate protein structures [13]. Both the species showed almost similar secondary structures with few changes (Table 1). *A. fabrum* possesses an extra helix whereas *B. subtilis* showed a higher presence of beta bulge, strands, and beta turns. Compact molecules are produced via β -turns in polypeptide chains, which are stabilized by hydrogen bonds. Beta bulges are introduced to prevent β -strand aggregation and are involved in protein-protein interactions.

Table 1. Secondary structure assessment of imidazolonepropionase from *Agrobacterium fabrum* and *Bacillus subtilis*.

Name	Sheets	Beta-Alpha-Beta	Beta Hairpins	Beta Bulges	Strands	Helices	Helix-Helix Interacs	Beta Turns	Gamma Turns
<i>Agrobacterium fabrum</i>	2	7	4	7	16	19	21	21	6
<i>Bacillus subtilis</i>	2	7	4	8	17	18	21	22	6

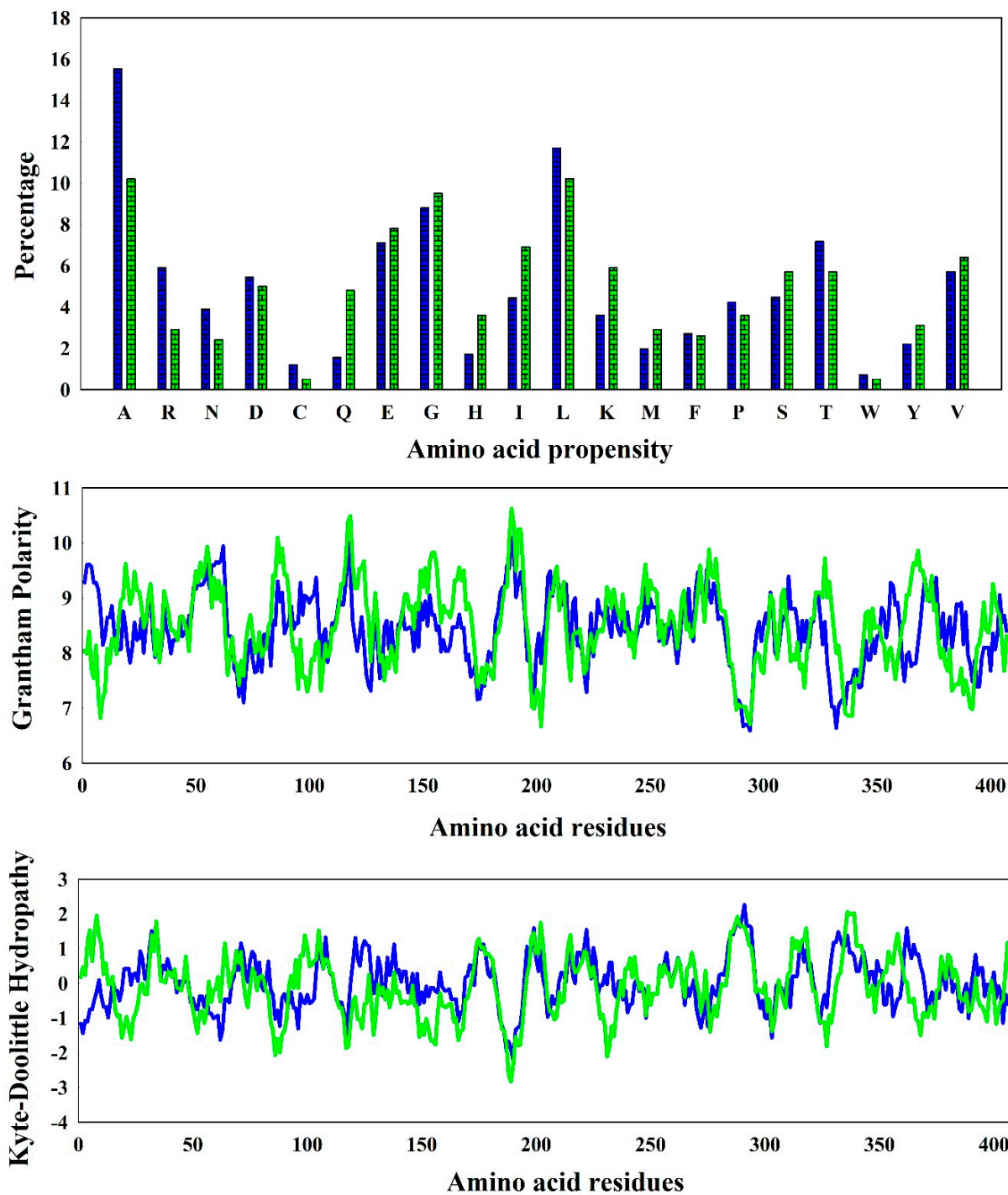


Figure 2. Amino acid diversity, Grantham polarity, and Kyte-Doolittle hydropathy of imidazolonepropionase from *Agrobacterium fabrum* (blue) and *Bacillus subtilis* (green).

3.2. Formation of Intra-Protein Interactions

In proteins, intra-residue interactions are crucial because they affect how the backbone folds locally. An interaction between two groups of opposing charges is known as a salt bridge when at least one pair of heavy atoms is within hydrogen bonding distance. Although the impact varies depending on the surroundings, salt bridges can help maintain the stability of proteins. Predicting salt bridge interactions is particularly difficult because of the high cost of dehydrating a basic residue and a carboxylate to create a salt bridge and the strict geometric constraints imposed by the electrostatic and hydrogen-bonding interactions [12]. Although the no. of isolated salt bridges was higher in *A. fabrum* (Table 2). To overcome these lacunae *B. subtilis* formed 3 network salt bridges which provide more stability for the protein. Not only the salt bridges, similar results were also found in the case of aromatic-aromatic interactions. The no. of isolated aromatic-aromatic interactions was slightly high in imidazolonepropionase from *A. fabrum*. But again, *B. subtilis* formed 5 network aromatic-aromatic interactions. The higher beta-turn helps to increase the network intra-protein interactions. So, imidazolonepropionase from *B. subtilis* focused on the formation of more network intra-protein interactions to enhance its stability in adverse conditions.

Table 2. Intra-protein interactions of imidazolonepropionase from *Agrobacterium fabrum* and *Bacillus subtilis*.

Name	Salt Bridge		Aromatic-Aromatic		Cation-Pi	
	Isolated	Network	Isolated	Network	Isolated	Network
<i>Agrobacterium fabrum</i>	19	0	3	2	4	0
<i>Bacillus subtilis</i>	13	3	2	5	4	0

3.3. Stability Checks Through Simulation Studies

Molecular dynamics simulations have developed into a sophisticated method that is useful for comprehending the links between macromolecular structure and function. Current simulation times are not too far from those that are important to biology. The amount of data acquired on the dynamic characteristics of macromolecules is sufficient to change the conventional paradigm of structural bioinformatics from single-structure analysis to conformational ensemble analysis [14]. One of the most practical and simple properties for structural comparison between the same protein of different species is the root mean square deviation, or RMSD [15]. Imidazolonepropionase from *B. subtilis* showed lower RMSD than *A. fabrum* (Figure 3). Both the species started from the same point but after 8 ns, *B. subtilis* went upward and ended at 0.26 nm.

An extremely flexible or unstructured portion of a protein may be identified using a Root-mean-square fluctuation (RMSF) plot, which displays the mean fluctuation of each amino acid throughout the simulation [16]. The quantity of fluctuations was high in imidazolonepropionase from *A. fabrum*. It showed very high fluctuations at residues no. 30, 105, 200, and 310. Imidazolonepropionase from *B. subtilis* showed fluctuations at 80 and 315. So, the imidazolonepropionase from *B. subtilis* was more stable than *A. fabrum*.

A polypeptide's radius of gyration (Rg) can serve as a crucial indicator of the equilibrium unfolding response as it unfolds. Higher Rg protein structures are often more stretched and flexible, whereas lower Rg protein structures are typically more globular and compact [17]. The Rg of imidazolonepropionase from *B. subtilis* showed a slightly lower value which indicates that it was more compact than *A. fabrum*.

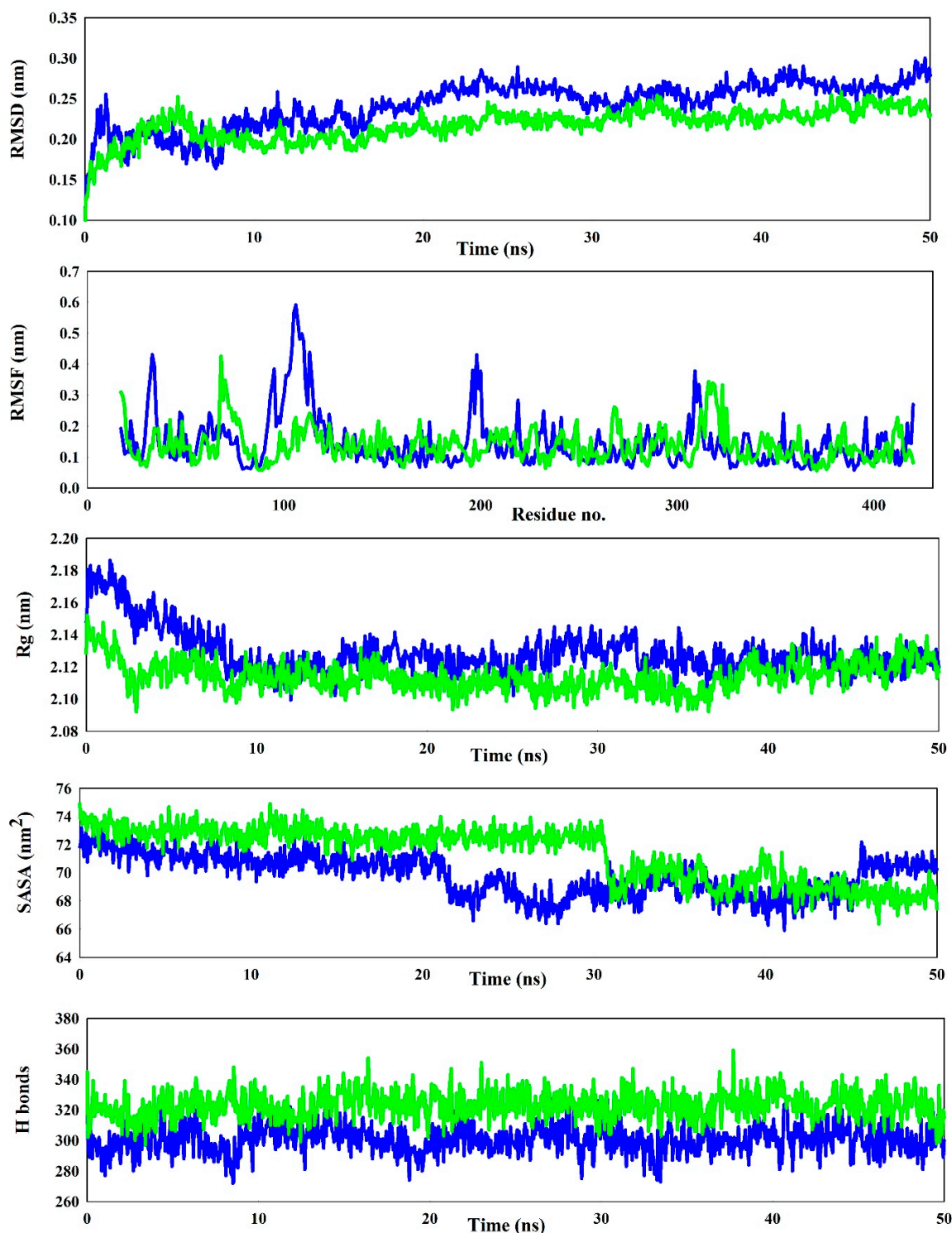


Figure 3. RMSD, RMSF, Rg, SASA and H-bonds of imidazolonepropionase from *Agrobacterium fabrum* (blue) and *Bacillus subtilis* (green).

Analysis of solvent-accessible surface area (SASA) is crucial to both biophysical chemistry and structural biology. It offers a crucial foundation for comprehending the molecular relationships, stability, and functionality of DNA, RNA, and proteins. Predicting molecular behaviour, including ligand binding, protein folding, and protein-protein interactions, requires a fundamental understanding of SASA [18]. Induced SASA values frequently mean that a protein has been exposed to a solvent, which might improve its flexibility and make drug binding easier. Up to 30 ns, imidazolonepropionase from *B. subtilis* showed

higher SASA than *A. fabrum*. Suddenly after that, it went downward and showed a lower value than *A. fabrum* and ended at 68 nm². So, imidazolonepropionase from *A. fabrum* has a higher tendency to react with ligands and ions.

One important aspect of protein structure is hydrogen bonding. They happen anytime two electronegative atoms share a proton, according to the widely accepted definition [19]. The no. of hydrogen bond formation was very high in imidazolonepropionase of *B. subtilis* rather than *A. fabrum*. So, these hydrogen bonds have a huge contribution to the protein stability of *B. subtilis*.

4. Conclusions

The third stage in the universal histidine degradation route is catalysed by imidazolonepropionase, which hydrolyses the carbon-nitrogen bonds in 4-imidazolone-5-propionic acid to produce N-formimino-L-glutamic acid. This in silico study has revealed the difference between the same enzyme in different bacterial species. Imidazolonepropionase of *B. subtilis* incorporated more charged amino acids in its sequence which further enhanced protein stability by increasing the enzyme polarity and hydrophilicity. Secondary structure assessment exposed that the imidazolonepropionase of *B. subtilis* had higher no. of beta bulge, strands, and beta turns. Instead of the formation of isolated intra-protein interactions, imidazolonepropionase of *B. subtilis* formed a higher network of intra-protein interactions. Molecular dynamics simulation revealed that imidazolonepropionase of *B. subtilis* had a more stable, less fluctuated, and more compact protein structure rather than *A. fabrum*.

Author Contributions: Conceptualization, D.M. and I.B.; methodology, I.B. and T.B.; software, D.M.; validation, D.M.; formal analysis, I.B.; investigation, D.M.; resources, D.M.; data curation, I.B.; writing original draft preparation, I.B. and T.B.; writing—review and editing, D.M.; visualization, I.B.; supervision, D.M. All authors have read and agreed to the published version of the manuscript.

Funding: This research received no external funding.

Institutional Review Board Statement: Not applicable.

Informed Consent Statement: Not applicable.

Data Availability Statement: Data are contained within the article.

Conflicts of Interest: The authors declare no conflicts of interest.

References

1. Tyagi, R.; Kumaran, D.; Burley, S.; Swaminathan, S. X-ray structure of imidazolonepropionase from *Agrobacterium tumefaciens* at 1.87 angstrom resolution. *Proteins Struct. Funct. Bioinform.* **2007**, *69*, 652–658. [[CrossRef](#)] [[PubMed](#)]
2. Yu, Y.; Liang, Y.H.; Brostromer, E.; Quan, J.M.; Panjekar, S.; Dong, Y.H.; Su, X.D. A catalytic mechanism revealed by the crystal structures of the imidazolonepropionase from *Bacillus subtilis*. *J. Biol. Chem.* **2006**, *281*, 36929–36936. [[CrossRef](#)] [[PubMed](#)]
3. Tyagi, R.; Eswaramoorthy, S.; Burley, S.K.; Raushel, F.M.; Swaminathan, S. A common catalytic mechanism for proteins of the HutI family. *Biochemistry* **2008**, *47*, 5608–5615. [[CrossRef](#)] [[PubMed](#)]
4. Snyder, S.H.; Silva, O.L.; Kies, M.W. The mammalian metabolism of L-Histidine: IV. purification and properties of imidazolone propionic acid hydrolase. *J. Biol. Chem.* **1961**, *236*, 2996–2998. [[CrossRef](#)] [[PubMed](#)]
5. Yu, Y.; Li, L.; Zheng, X.; Liang, Y.H.; Su, X.D. Protein preparation, crystallization and preliminary X-ray analysis of imidazolonepropionase from *Bacillus subtilis*. *Biochim. Biophys. Acta (BBA)-Proteins Proteom.* **2006**, *1764*, 153–156. [[CrossRef](#)] [[PubMed](#)]
6. Yang, F.; Chu, W.; Yu, M.; Wang, Y.; Ma, S.; Dong, Y.; Wu, Z. Local structure investigation of the active site of the imidazolonepropionase from *Bacillus subtilis* by XANES spectroscopy and ab initio calculations. *J. Synchrotron Radiat.* **2008**, *15*, 129–133. [[CrossRef](#)] [[PubMed](#)]
7. Gasteiger, E.; Hoogland, C.; Gattiker, A.; Duvaud, S.E.; Wilkins, M.R.; Appel, R.D.; Bairoch, A. *Protein Identification and Analysis Tools on the ExPASy Server*; Humana Press: Totowa, NJ, USA, 2005; pp. 571–607.

8. Mitra, D.; Pal, A.K.; Das Mohapatra, P.K. Intra-protein interactions of SARS-CoV-2 and SARS: A bioinformatic analysis for plausible explanation regarding stability, divergency, and severity. *Syst. Microbiol. Biomanuf.* **2022**, *2*, 653–664. [[CrossRef](#)] [[PubMed](#)]
9. Mitra, D.; Das Mohapatra, P.K. In silico comparative structural compositional analysis of glycoproteins of RSV to study the nature of stability transmissibility of RSV A. *Syst. Microbiol. Biomanuf.* **2023**, *3*, 312–327. [[CrossRef](#)] [[PubMed](#)]
10. Abraham, M.J.; Murtola, T.; Schulz, R.; Páll, S.; Smith, J.C.; Hess, B.; Lindahl, E. GROMACS: High performance molecular simulations through multi-level parallelism from laptops to supercomputers. *SoftwareX* **2015**, *1*, 19–25. [[CrossRef](#)]
11. Díaz-Pascual, F.; Lempp, M.; Nosh, K.; Jeckel, H.; Jo, J.K.; Neuhaus, K.; Hartmann, R.; Jelli, E.; Hansen, M.F.; Price-Whelan, A.; et al. Spatial alanine metabolism determines local growth dynamics of Escherichia coli colonies. *Elife* **2021**, *10*, e70794. [[CrossRef](#)] [[PubMed](#)]
12. Mitra, D.; Das Mohapatra, P.K. Discovery of novel cyclic salt bridge in thermophilic bacterial protease and study of its sequence and structure. *Appl. Biochem. Biotechnol.* **2021**, *193*, 1688–1700. [[CrossRef](#)] [[PubMed](#)]
13. Biswas, I.; Mitra, D. In silico sequence-structure based analysis of bacterial chromate reductase to unravel enzymatic specificity towards chromium pollution. *Biocatal. Agric. Biotechnol.* **2024**, *60*, 103339. [[CrossRef](#)]
14. Hospital, A.; Goñi, J.R.; Orozco, M.; Gelpí, J.L. Molecular dynamics simulations: Advances and applications. *Adv. Appl. Bioinform. Chem.* **2015**, *8*, 37–47. [[PubMed](#)]
15. Mitra, D.; Afreen, S.; Das Mohapatra, P.K.; Abdalla, M. Threat of respiratory syncytial virus infection knocking the door: A proposed potential drug candidate through molecular dynamics simulations, a future alternative. *J. Mol. Model.* **2023**, *29*, 91. [[CrossRef](#)] [[PubMed](#)]
16. Biswas, I.; Mitra, D. November. Comparative Analysis of RuBisCO Evolution and Intrinsic Differences: Insights from In Silico Assessment in Cyanobacteria, Monocot, and Dicot Plants. *Biol. Life Sci. Forum* **2023**, *27*, 44.
17. Mitra, D.; Afreen, S.; Das Mohapatra, P.K.; Abdalla, M. Inhibition of respiratory syncytial virus by Daclatasvir and its derivatives: Synthesis of computational derivatives as a new drug development. *J. Biomol. Struct. Dyn.* **2025**, *43*, 2440–2462. [[CrossRef](#)] [[PubMed](#)]
18. Mitra, D.; Paul, M.; Thatoi, H.; Das Mohapatra, P.K. Potentiality of bioactive compounds as inhibitor of M protein and F protein function of human respiratory syncytial virus. *Silico Pharmacol.* **2023**, *12*, 5. [[CrossRef](#)] [[PubMed](#)]
19. Derewenda, Z.S.; Lee, L.; Derewenda, U. The occurrence of C–H···O hydrogen bonds in proteins. *J. Mol. Biol.* **1995**, *252*, 248–262. [[CrossRef](#)]

Disclaimer/Publisher’s Note: The statements, opinions and data contained in all publications are solely those of the individual author(s) and contributor(s) and not of MDPI and/or the editor(s). MDPI and/or the editor(s) disclaim responsibility for any injury to people or property resulting from any ideas, methods, instructions or products referred to in the content.